

Gradient is All You Need: Gradient-Based Attention Fusion for Infrared Small Target Detection

Chen Hu, Yian Huang, *Student Member, IEEE*, Kexuan Li, Luping Zhang, Yiming Zhu, Yufei Peng, Tian Pu, and Zhenming Peng, *Member, IEEE*

Abstract—Infrared small target detection (IRSTD) is widely used in civilian and military applications. However, IRSTD encounters several challenges, including the tendency for small and dim targets to be obscured by complex backgrounds. To address this issue, we propose the Gradient Network (GaNet), which aims to extract and preserve edge and gradient information of small targets. GaNet employs the Gradient Transformer (GradFormer) module, simulating central difference convolutions (CDC) to extract and integrate gradient features with deeper features. Furthermore, we propose a global feature extraction model (GFEM) that offers a comprehensive perspective to prevent the network from focusing solely on details while neglecting the background information. We compare the network with state-of-the-art (SOTA) approaches, and the results demonstrate that our method performs effectively. Our source code is available at <https://github.com/greekinRoma/Gradient-Transformer>.

Index Terms—Infrared small target detection (IRSTD), convolution neural network (CNN), gradient Transformer, global feature extraction.

I. INTRODUCTION

INFRARED small target detection (IRSTD) is critically important for numerous space-based computer vision applications, including remote sensing [1], precision guidance [2], and marine rescue [3]. While IRSTD has been extensively studied, it remains challenging. The considerable imaging distances associated with space-based infrared cameras often result in small targets that lack detailed texture and shape information.

Currently, the IRSTD methods can be categorized into model-driven and data-driven methods. Model-driven methods include three main approaches. 1) Filter-based methods, such as the Top-hat [4] and Max-Median filters [5], enhance the target visibility in complex backgrounds while suppressing background noise. 2) Human visual system (HVS)-based methods,

such as the local contrast measure (LCM) [6] and multi-patch contrast measure (MPCM) [7], leverage human visual perception to enhance local information. 3) Low-rank matrix decomposition and reconstruction methods, such as infrared patch-image (IPI) [8] and reweight image patch tensor (RIPT) [9], decompose small targets and backgrounds using low-rank matrices. However, these techniques require manual parameter settings and often need help to adapt to complex scenarios, particularly in high noise levels or significant background clutter.

With the advancement of deep learning, data-driven approaches have achieved substantial progress in infrared small target detection (IRSTD). For example, the Asymmetric Context Modulation (ACM) network [10] introduces an asymmetric feature fusion technique, an alternative to the conventional skip connections in U-Net. Building on this, DNANet [11] implements a multi-layer nested architecture that supports progressive and adaptive interactions among feature layers. Moreover, UTUNet [12] enhances the detection of local target contrasts by integrating multiple U-Net structures and utilizing interactive cross-attention mechanisms for feature fusion. Additionally, GSTUNet [13] merges vision Transformer technology with CNNs in the encoder to efficiently extract edge features from small targets. Generally, these data-driven methods surpass traditional model-driven approaches. However, they have drawbacks, such as the substantial number of parameters and the potential loss of local feature information in higher layers, indicating opportunities for further enhancements.

In order to address the challenges of feature extraction, we propose the Gradient Attention Network (GaNet). GaNet incorporates two key innovation components to improve feature extraction. First, we propose a gradient Transformer (GradFormer) module that performs the feature gradient calculations by simulating the central difference convolutions (CDC) and enhances weak features to enable the network to learn a comprehensive feature representation of the target. Second, the global feature extraction module (GFEM) solves the problem of lacking global background perception, thereby improving the ability to obtain contextual information. The main contributions of this letter are as follows.

- 1) We propose the GaNet, which utilizes the GradFormer to simulate the CDC with dynamic weights, extracting the edge and point information vital for IRSTD.
- 2) We propose the GFEM to improve the CNN from only focusing on local details to integrating these details with global information.
- 3) We conduct comparative experiments on the IRSTD-1K

Manuscript received XXX XXX, XXX; revised XXX XXX, XXX.

This work was supported by the National Natural Science Foundation of China (Grant No.61775030 and Grant No.61571096). (*Corresponding authors: Zhenming Peng; Tian Pu.*)

Chen Hu, Yian Huang, Kexuan Li, Yufei Peng, Luping Zhang, Tian Pu, and Zhenming Peng are with the Laboratory of Imaging Detection and Intelligent Perception and the School of Information and Communication Engineering, University of Electronic Science and Technology of China, Chengdu 610054, China (e-mail: 202221011506@std.uestc.edu.cn; huangyian@std.uestc.edu.cn; 202322011823@std.uestc.edu.cn; anguing@foxmail.com; feifyaoqifei@gmail.com; putian@uestc.edu.cn; zmpeng@uestc.edu.cn)

Yiming Zhu is with School of Computer Science and Engineering, Nanjing University of Science and Technology, Nanjing, China. (e-mail: yiming_zhu_grokc@163.com)

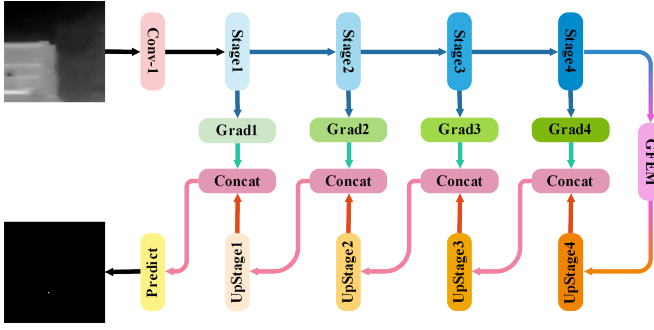


Fig. 1. The overall structure of GaNet. The blue represents the downsampling module, the green indicates the GradFormer module, the orange corresponds to the upsampling module, the red signifies the concatenate operation, and the purple denotes the global feature extraction module (GFEM).

and NUDT-SIRST datasets, and the results show that GaNet outperforms existing methods.

II. METHODS

The overall architecture of GaNet is illustrated in Fig. 1. GradFormer is utilized to extract gradient information, and GFEM enhances contextual features. Finally, detailed information from low-level layers is integrated with high-level semantics with the global receptive field.

A. Gradient Transformer (GradFormer)

CDCs are defined in Eq. 1 and are employed to extract edge and gradient features. Here, c_i represents the number of input channels, o_{ixy} denotes the input value at the i -th channel and position (x, y) , and b_{ijxy} refers to the j -th surrounding value around o_{ixy} . While CDCs excel at extracting details, there is still room for improvement. A significant limitation is the use of fixed weights for different directions, meaning the importance of each direction remains constant across different images.

$$out_{cxy} = \sum_{i=0}^{c_i-1} \sum_{j=0}^7 w_{c_{ijxy}} (b_{ijxy} - o_{ixy}) \quad (1)$$

We can transform Eq. 1 into a fusion of Eq. 2 and Eq. 3. The process described in Eq. 2 is illustrated in Fig. 2. As shown in Fig. 2, we use edge convolution to extract the difference values from the input $T \in \mathbb{R}^{c_i \times w \times h}$ and reshape them to produce a local difference matrix $D \in \mathbb{R}^{8c_i \times wh}$. In Eq. 3, we utilize the weight matrix $M_w \in \mathbb{R}^{c_o \times 8c_i}$ and the local difference matrix D to obtain the final result Out . Here, w denotes the width of the input, h represents the input height, and c_o signifies the number of output channels.

$$D = \text{reshape}(\text{Conv}_{3 \times 3}(T)) \quad (2)$$

$$Out = M_w D \quad (3)$$

When M_w is influenced by the input T_i , the CDC could exhibit enhanced robustness. Based on the analysis above, we introduce the GradFormer to simulate CDC and extract

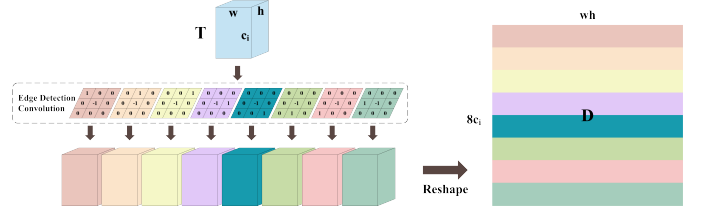


Fig. 2. D is obtained by performing edge detection convolution on T_i and unfolding the output.

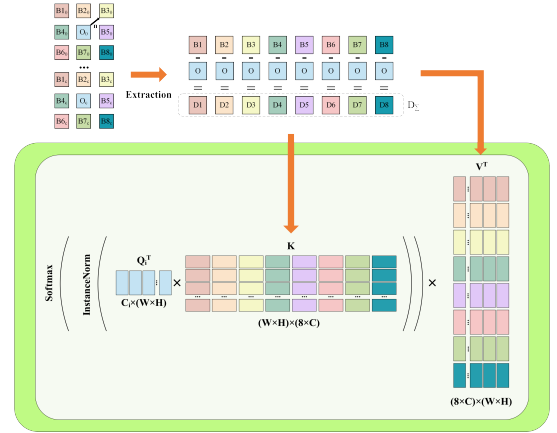


Fig. 3. The various heads in GradFormer employ the edge convolution to get D_{Σ} . Each head's key and value are derived from D_{Σ} , while the query is generated from the flattened input.

the details using dynamic weights from low-level layers for IRSTD. The structure of GradFormer is shown in Fig. 3.

In varied heads of the GradFormer, we employ different unfolding methods based on edge detection convolutions in Fig. 2 with varying dilation and reshape operations to get the unfolding.

In the various heads of GradFormer, we apply different edge detection convolutions from Fig. 2 to T , utilizing varying dilation ratios. The outputs from these convolutions are then reshaped into $D^n \in \mathbb{R}^{8c_i \times wh}$. Additionally, the input T is reshaped to form $O \in \mathbb{R}^{c_i \times wh}$. The token O serves as the query, and the local difference matrix $D^n \in \mathbb{R}^{8c_i \times wh}$ functions as both the key and the value.

$$Q^n = W_Q^n O, K^n = W_K^n D^n, V = W_V^n D^n \quad (4)$$

where $W_Q^n \in \mathbb{R}^{\frac{c_o}{m} \times c_i}$, $W_K^n \in \mathbb{R}^{\frac{8c_i}{m} \times 8c_i}$, $W_V^n \in \mathbb{R}^{\frac{8c_i}{m} \times 8c_i}$ are the reshaped weights of convolutions, n denotes dilation ratios, and m denotes the number of heads. We utilize the $Q^n \in \mathbb{R}^{\frac{c_o}{m} \times wh}$ and $K^n \in \mathbb{R}^{\frac{8c_i}{m} \times wh}$ to produce the attention matrix $M^n \in \mathbb{R}^{\frac{c_o}{m} \times \frac{8c_i}{m}}$. $V^n \in \mathbb{R}^{\frac{8c_i}{m} \times wh}$ denotes the value of the transformer. The result $Out^n \in \mathbb{R}^{\frac{c_o}{m} \times wh}$ is defined as follows:

$$\begin{aligned} Out^n &= \text{Softmax}(\text{Norm}(\frac{Q^n (K^n)^T}{w})) V^n \\ &= M^n V^n = (M^n W_V^n) D^n = M_{mix}^n D^n \end{aligned} \quad (5)$$

where $M_{mix}^n \in \mathbb{R}^{\frac{c_o}{m} \times 8c_i}$ denotes the dynamic matrix derived from an attention matrix M^n and a fixed convolution weight matrix W_V^n . According to Eq. 3, Out^n is the equivalent result

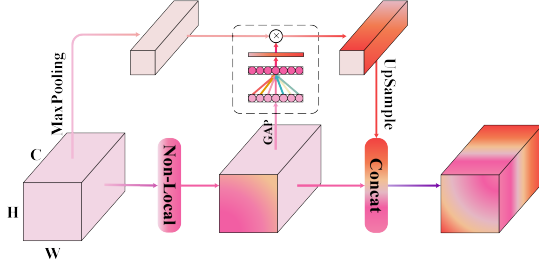


Fig. 4. Diagram of the Global Feature Extraction Module (GFEM) using the Non-local Attention Module to capture global spatial features and Squeeze-and-Excitation Block to extract global channel information.

of the CDC with dynamic weights and a dilation ratio of n . $Norm$ is the Instance Normalization. At last, we concatenate the results in varied heads, reshape them and use 1×1 convolution to fuse them as shown in the Equation below:

$$Out = Conv_{1 \times 1}(reshape(Out^1, \dots, Out^m)) \quad (6)$$

Overall, the gradient information from features at different scales can be fully extracted, enhancing the model's ability to adapt to complex backgrounds.

B. Global Feature Extraction Module

Background information is crucial alongside detailed features inIRSTD. However, perceiving background relies on global features, which the GradFormer struggles to handle effectively. To address this limitation and enhance global information perception, we propose the Global Feature Enhancement Module (GFEM), as illustrated in Fig. 4.

In GFEM, we utilize the attention mechanism to facilitate the transmission of information across distant pixels. This module includes two key aspects to broaden perception: First, we employ the non-local attention mechanism [14] to compute the spatial attention, enabling connectivity between pixels over long distances. Second, we incorporate a squeeze-and-excitation block [15] to enhance channel-wise perception. Finally, we concatenate the outputs from the global spatial and channel attention modules and apply convolution to fuse them, enabling GFEM to capture comprehensive feature representations.

Subsequently, each feature map acquires both spatial and channel global receptive fields, which are vital for effective object detection.

C. Loss Function

The loss function utilized in our model training is the soft intersection over union (SoftIoU) loss, where the predictions of GaNet are mapped into the range of 0 and 1, using the Sigmoid function as shown in Eq. 7.

$$p_{i,j} = \frac{1}{1 + e^{-v_{i,j}}} \quad (7)$$

where $p_{i,j}$ denotes the Sigmoid output of $v_{i,j}$, the model's prediction at pixel (i, j) . Moreover, the SoftIoU loss is defined as:

$$SoftIoU = 1 - \frac{\sum_{i,j} p_{i,j} \cdot g_{i,j}}{\sum_{i,j} p_{i,j} + \sum_{i,j} g_{i,j} - \sum_{i,j} p_{i,j} \cdot g_{i,j}} \quad (8)$$

$$SoftIoU_{loss} = 1 - SoftIoU \quad (9)$$

In this equation, $g_{i,j}$ denotes the ground truth value at pixel (i, j) , typically 0 or 1.

III. EXPERIMENT AND ANALYSIS

This section describes the experimental details, including a series of ablation studies to verify the proposed modules. Comparative experiments with other methods demonstrate that our approach outperforms existing state-of-the-art (SOTA) methods.

A. Dataset and Evaluation Metrics

The datasets used for evaluating the GaNet are NUDT-SIRST [11] andIRSTD-1k [16], which are widely employed to assess model performance. The evaluation metrics include mean intersection over union ($mIoU$), F-measure (F_1), the probability of detection (P_d), and false alarm rate (F_a).

B. Experimental Environment and Parameter Settings

Our model is implemented by the PyTorch framework on NVIDIA GeForce RTX 4080 GPUs. We employ the Adam optimizer, starting with an initial learning rate of 5×10^{-4} . This learning rate is reduced to 5×10^{-5} at epoch 200 and further decrease to 5×10^{-6} . We use a batch size of 4 for training and run the model for 400 epochs.

C. Ablation Study

TABLE I
STUDIES ON DIFFERENT DILATION RATES ON NUDT-SIRST (THE BEST RESULTS ARE BOLD)

Dilation Rate	mIoU(%)	F_1 (%)	P_d (%)	$F_a(10^{-6})$
1	93.53	96.30	98.89	5.58
1,3	94.82	97.34	98.94	1.82
1,5	94.24	97.03	98.65	1.47

TABLE II
STUDIES OF DIFFERENT COMPONENTS ON NUDT-SIRST (THE BEST RESULTS ARE BOLD)

Module	mIoU(%)	F_1 (%)	P_d (%)	$F_a(10^{-6})$
U-Net	91.31	95.44	97.98	4.46
U-Net+GradFormer	94.25	97.03	98.83	2.73
U-Net+GFEM	92.32	96.14	96.30	3.96
U-Net+GradFormer+GFEM	94.82	97.34	98.94	1.82

1) *Studies of Dilation Rate for GradFormer:* As mentioned in II-A, GradFormer employs varying dilation rates across different heads. Tab. I demonstrates the efficacy of this strategy, as models featuring diverse dilation ratios outperform those with a uniform rate. Furthermore, networks employing dilation ratios of 1 and 3 yield superior results compared to those with larger ratios, indicating that smaller dilation ratios are more effective for capturing local differences in infrared small targets, likely due to their small size. Therefore, the dilation ratio significantly impacts target detection, making its configuration crucial for the effectiveness of GradFormer.

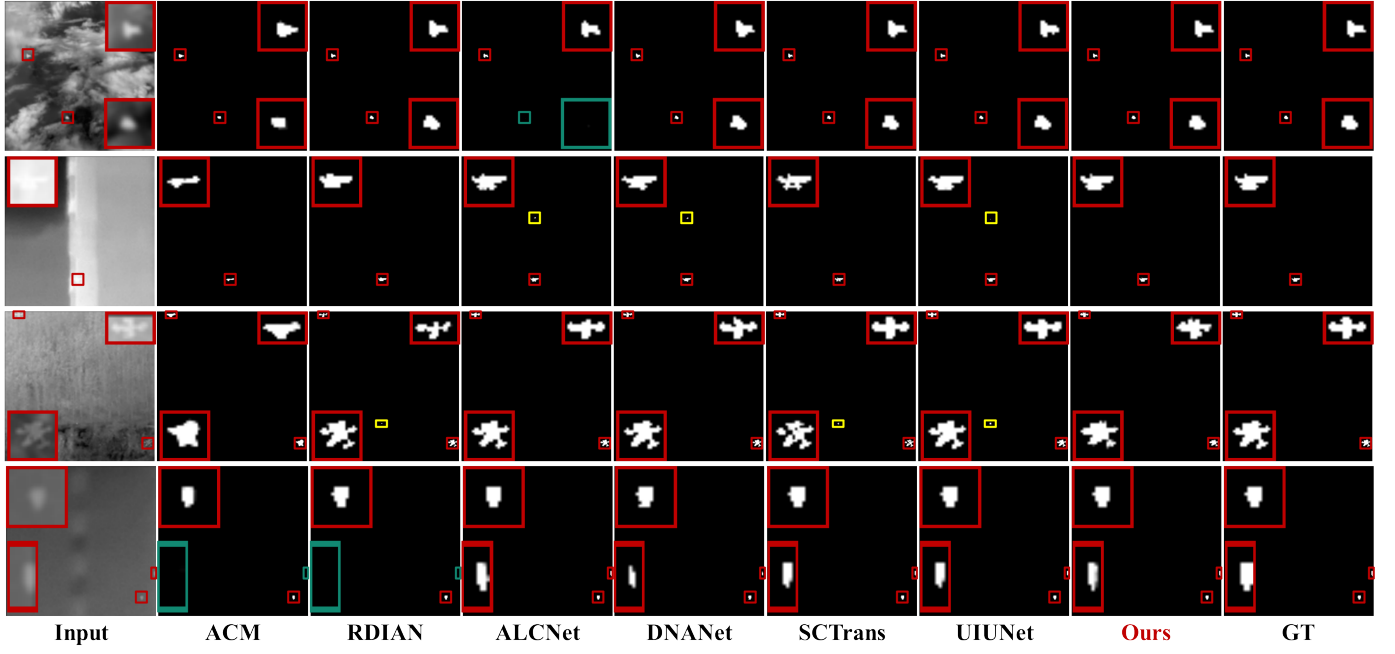


Fig. 5. Visual results from varied data-driven methods. Red, green, and yellow boxes label detected targets, missed targets, and false alarms.

TABLE III
QUANTITATIVE COMPARISON WITH DIFFERENT METHODS (THE BEST RESULTS ARE **BOLD**, SECOND BEST RESULTS ARE UNDERLINE.)

Module	Metrics Params(M)	NUDT-SIRST				IRSTD1K			
		mIoU(%)	F_1 (%)	P_d (%)	$P_a(10^{-6})$	mIoU(%)	F_1 (%)	P_d (%)	$P_a(10^{-6})$
ACM [10]	0.40	69.69	82.10	96.82	8.12	63.78	77.91	93.93	5.81
RDIAN [17]	0.90	86.67	93.81	97.98	4.76	64.08	78.12	93.34	5.30
ALCNet [18]	0.37	92.39	96.04	98.83	3.79	65.10	78.88	93.26	7.90
AGPCNet [19]	13.36	86.71	92.88	98.09	3.93	67.54	80.64	<u>94.27</u>	4.76
DNANet [11]	4.69	93.41	96.59	<u>98.94</u>	3.52	65.79	79.23	93.60	5.96
UIU-Net [12]	50.54	<u>94.27</u>	<u>97.04</u>	98.73	1.22	68.06	<u>80.91</u>	92.59	5.85
SCTransNet [20]	11.19	93.38	96.57	97.88	4.73	67.97	80.90	93.26	6.24
Ours	4.46	94.82	97.34	98.94	<u>1.82</u>	68.26	81.11	95.95	4.42

2) *Studies of Various Components*: We illustrate the effectiveness of each module in Tab. II. The performance of our network improves progressively with the inclusion of each module. GradFormer, which focuses on local difference features, enhances the model's performance more effectively than GFEM, which primarily relies on global perception. In IRSTD, the capability to learn gradient information is more critical than access to global context.

D. Comparison with State-of-the-art (SOTA) Methods

To demonstrate the effectiveness of our proposed model, we compare it with several SOTA methods on two datasets, including SCTransNet [20], UIUNet [12], ACM [10], ALCNet [18], AGPCNet [19], RDIAN [17], and DNANet [11]. As shown in Tab. III, and our method performs excellently. We utilize GaNet with dilation ratios of 1 and 5 as the baseline models for comparative evaluation.

1) *Qualitative Result*: As shown in Fig. 5, our model preserves the shape of targets with low missed detections (green boxes) and false alarms (yellow boxes) compared to other methods. Our approach excels in learning rich feature

representations by seamlessly integrating detailed features with high-level semantics and leveraging a global attention, which enables precise differentiation between targets and backgrounds, effectively mitigating false alarms and reducing missed detections. Despite the challenges posed by small and dim targets in infrared images with complex backgrounds, our network consistently balances segmentation quality with detection accuracy. While methods like UIU-Net may retain target structure, they often suffer from false positives and negatives. Other approaches, such as ALCNet, may exhibit fewer false alarms and missed targets but struggle to maintain target shapes. Through comparisons with other methods, we have highlighted the superior performance of our approach.

2) *Quantitative Results*: As shown in Tab. III, our method achieves impressive performance, including an $mIoU$ of 95.21%, an $F1$ score of 97.51%, and a Pd of 99.04%, a Pa of 1.06×10^{-6} . With 4.46M parameters, it is significantly more efficient than other methods. Similarly, on the IRSTD-1k dataset, our method is a leading network. Generally, methods that rely on data with more complex structures tend to perform better. However, our network demonstrates that such models often extract features that are irrelevant to IRSTD. Instead, we

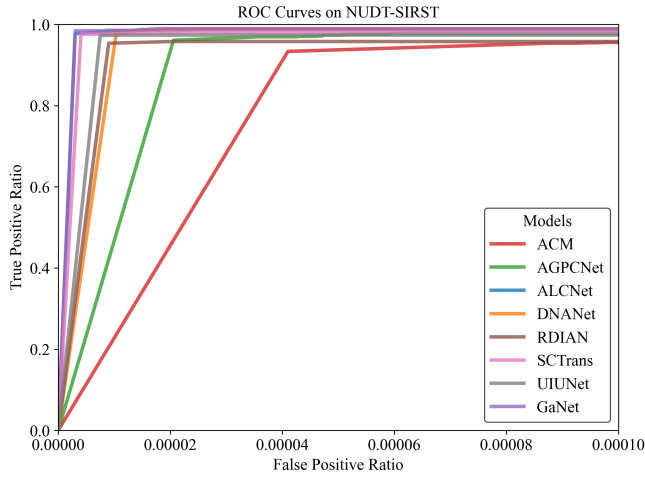


Fig. 6. ROC curves of varied networks on NUDT-SIRST.

focus on utilizing gradients from lower layers and semantics from deeper layers for optimal performance. Additionally, we employ the ROC curve to analyze the performance of various models, as depicted in Fig. 6. While UIU-Net achieves commendable results in $mIoU$, its AUC scores are comparatively weak. In contrast, ALCNet's performance shows significant divergence, with subpar outcomes in $mIoU$ but relatively strong performance in ROC metrics. The model proposed in this article consistently demonstrates good performance in both ROC and $mIoU$.

IV. CONCLUSION

In this letter, we propose an IRSTD network that enhances detection performance compared to baseline models and has fewer model parameters. The GradFormer module was proposed to improve the detection performance of the network. Additionally, we propose the GFEM module, which focuses on global perception across the entire feature map and learns relationships between distant pixels, preventing GradFormer from overlooking background information due to its emphasis on local differences. To demonstrate the effectiveness of the proposed network and modules, we conducted extensive experiments that indicate satisfied results and significant practical application potential.

REFERENCES

- [1] Jiehua Lin, Yan Zhao, Shigang Wang, and Yu Tang. Yolo-da: An efficient yolo-based detector for remote sensing object detection. *IEEE Geoscience and Remote Sensing Letters*, 2023.
- [2] Qingyu Hou, Zhipeng Wang, Fanjiao Tan, Ye Zhao, Haoliang Zheng, and Wei Zhang. Ristdnet: Robust infrared small target detection network. *IEEE Geoscience and Remote Sensing Letters*, 19:1–5, 2021.
- [3] Tianhao Wu, Boyang Li, Yihang Luo, Yingqian Wang, Chao Xiao, Ting Liu, Jungang Yang, Wei An, and Yulan Guo. Mtu-net: Multilevel transunet for space-based infrared tiny ship detection. *IEEE Transactions on Geoscience and Remote Sensing*, 61:1–15, 2023.
- [4] Xiangzhi Bai and Fugen Zhou. Analysis of new top-hat transformation and the application for infrared dim small target detection. *Pattern Recognition*, 43(6):2145–2156, 2010.
- [5] Suyog D Deshpande, Meng Hwa Er, Ronda Venkateswarlu, and Philip Chan. Max-mean and max-median filters for detection of small targets. In *Signal and Data Processing of Small Targets 1999*, volume 3809, pages 74–83. SPIE, 1999.

- [6] CL Philip Chen, Hong Li, Yantao Wei, Tian Xia, and Yuan Yan Tang. A local contrast method for small infrared target detection. *IEEE transactions on geoscience and remote sensing*, 52(1):574–581, 2013.
- [7] Yantao Wei, Xinge You, and Hong Li. Multiscale patch-based contrast measure for small infrared target detection. *Pattern Recognition*, 58:216–226, 2016.
- [8] Chenqiang Gao, Deyu Meng, Yi Yang, Yongtao Wang, Xiaofang Zhou, and Alexander G Hauptmann. Infrared patch-image model for small target detection in a single image. *IEEE transactions on image processing*, 22(12):4996–5009, 2013.
- [9] Yimian Dai and Yiquan Wu. Reweighted infrared patch-tensor model with both nonlocal and local priors for single-frame small target detection. *IEEE journal of selected topics in applied earth observations and remote sensing*, 10(8):3752–3767, 2017.
- [10] Yimian Dai, Yiquan Wu, Fei Zhou, and Kobus Barnard. Asymmetric contextual modulation for infrared small target detection. In *Proceedings of the IEEE/CVF Winter Conference on Applications of Computer Vision*, pages 950–959, 2021.
- [11] Boyang Li, Chao Xiao, Longguang Wang, Yingqian Wang, Zaiping Lin, Miao Li, Wei An, and Yulan Guo. Dense nested attention network for infrared small target detection. *IEEE Transactions on Image Processing*, 2022.
- [12] Xin Wu, Danfeng Hong, and Jocelyn Chanussot. Uiu-net: U-net in u-net for infrared small object detection. *IEEE Transactions on Image Processing*, 32:364–376, 2022.
- [13] Yiming Zhu, Yong Ma, Fan Fan, Jun Huang, Kangle Wu, and Ge Wang. Towards accurate infrared small target detection via edge-aware gated transformer. *IEEE Journal of Selected Topics in Applied Earth Observations and Remote Sensing*, 2024.
- [14] Xiaolong Wang, Ross Girshick, Abhinav Gupta, and Kaiming He. Non-local neural networks. In *Proceedings of the IEEE conference on computer vision and pattern recognition*, pages 7794–7803, 2018.
- [15] Jie Hu, Li Shen, and Gang Sun. Squeeze-and-excitation networks. In *Proceedings of the IEEE conference on computer vision and pattern recognition*, pages 7132–7141, 2018.
- [16] Mingjin Zhang, Rui Zhang, Yuxiang Yang, Haichen Bai, Jing Zhang, and Jie Guo. Isnet: Shape matters for infrared small target detection. In *Proceedings of the IEEE/CVF Conference on Computer Vision and Pattern Recognition*, pages 877–886, 2022.
- [17] Heng Sun, Junxiang Bai, Fan Yang, and Xiangzhi Bai. Receptive-field and direction induced attention network for infrared dim small target detection with a large-scale dataset irdst. *IEEE Transactions on Geoscience and Remote Sensing*, 61:1–13, 2023.
- [18] Y. Dai, Y. Wu, F. Zhou, and K. Barnard. Attentional local contrast networks for infrared small target detection. *IEEE transactions on geoscience and remote sensing*, 59(11):9813–9824, 2021.
- [19] Tianfang Zhang, Lei Li, Siying Cao, Tian Pu, and Zhenming Peng. Attention-guided pyramid context networks for detecting infrared small target under complex background. *IEEE Transactions on Aerospace and Electronic Systems*, 2023.
- [20] Shuai Yuan, Hanlin Qin, Xiang Yan, Naveed Akhtar, and Ajmal Mian. Sctransnet: Spatial-channel cross transformer network for infrared small target detection. *IEEE Transactions on Geoscience and Remote Sensing*, 62:1–15, 2024.